

Echoes of the whispering land: interacting roles of vicariance and selection in shaping the evolutionary divergence of two *Calceolaria* (Calceolariaceae) species from Patagonia and Malvinas/Falkland Islands

Matías Cristian Baranzelli¹ · Andrea Cosacov¹ · Anahí Espíndola² · Maria del Rosario Iglesias¹ · Lauren M. Chan³ · Leigh A. Johnson⁴ · Alicia Noemí Sérsic^{1,5} 

Received: 6 February 2018 / Accepted: 24 April 2018
© Springer International Publishing AG, part of Springer Nature 2018

Abstract A key to understanding the origin and identity of young species lays on the knowledge of the Quaternary climatic oscillations' effect on gene flow and vicariance. Even though the effect of climatic fluctuations is relatively well understood for southern hemisphere plant species, little is known about their effect on the evolutionary histories of species from mainland and islands. Thus, we investigated whether Quaternary climate-driven fluctuations translated into lineage divergence and speciation, followed or not by climatic niche differentiation, in two allopatric plant species, *Calceolaria uniflora* and *C. fothergillii* from Patagonia and Malvinas/Falkland islands, respectively. We

Matías Cristian Baranzelli, Andrea Cosacov and Alicia Noemí Sérsic have contributed equally to this study and should be considered as co-first authors.

Electronic supplementary material The online version of this article (<https://doi.org/10.1007/s10682-018-9938-3>) contains supplementary material, which is available to authorized users.

✉ Alicia Noemí Sérsic
asersic@imbiv.unc.edu.ar

¹ Laboratorio de Ecología Evolutiva - Biología Floral, Instituto Multidisciplinario de Biología Vegetal (IMBIV), CONICET-Universidad Nacional de Córdoba, Dirección postal: Casilla de Correo 495, X5000ZAA Córdoba, Argentina

² Department of Biological Sciences, University of Idaho, Life Sciences South 252, 875 Perimeter Dr. MS3051, Moscow, ID 83844-3051, USA

³ Department of Biology, Pacific University, 2043 College Way, Forest Grove, OR 97116, USA

⁴ Department of Biology and M. L. Bean Life Science Museum, Brigham Young University, Provo, UT 84602, USA

⁵ Instituto Multidisciplinario de Biología Vegetal (IMBIV), Ciudad Universitaria, Av. Vélez Sársfield 1611, X5016GCA Córdoba, Argentina

sampled the range of both species, and sequenced two chloroplastic (cpDNA; *trnS-trnG* and *trnH-psbA*), and one single copy “anonymous” non-coding nuclear region (nDNA). We performed phylogeographic and dating analyses, and adjusted spatio-temporal diffusion models. We complemented molecular evidence with climatic niche differentiation analyses and species paleo-distribution projections. A species coalescent reconstruction based on multi-locus data retrieved both species as monophyletic. Estimates from cpDNA indicated the species diverged during the Great Patagonian Glaciation. Chloroplast and nuclear DNA showed east–west distribution of the main genetic groups but with contrasting spatial genetic diversity. The spatio-temporal diffusion analyses showed that between 1–0.8 Mya and 570 Kya the lineage leading to *C. fothergillii* diverged from *C. uniflora* and arrived to the islands. Climatic niche projections hindcasted range expansions during glaciations, and contractions during the interglacial periods. Comparisons of climatic niches between the two study species indicated that temperature variables show evidence of niche conservatism while precipitation regimes supported niche divergence, even when considering the background environmental divergence. Our study indicates that glacial fluctuations affected the mainland/islands connections favouring speciation mediated not only by isolation, but also by climatic niche differentiation.

Keywords Climatic niche differentiation · Gene flow · Paleo distribution models · Plant phylogeography · Pleistocene glaciations · Speciation

Introduction

Dramatic environmental changes associated with cycles of glaciation and deglaciation occurred in the Quaternary. These events have been credited with promoting lineage diversification that can lead to speciation worldwide (Comes and Kadereit 1998; Hewitt 2004; Rull 2006). Because species or lineages that became isolated on islands facilitates understanding the mechanisms underlying species formation (Losos and Ricklefs 2009), insights into the role of glaciations promoting speciation can be gained by studying allopatric sister species inhabiting mainland and islands whose connections were affected by Quaternary climatic fluctuations. For the Southern Hemisphere, range shifts and allopatric differentiation are relatively well-documented species responses to past climate change (e.g. Séršic et al. 2011), but whether these processes were accompanied by adaptation to different environments, promoting niche divergence and speciation, has been less widely explored (Camargo et al. 2010).

The evolutionary history of Patagonia has been marked by geologic and climatic events that occurred in the past several million years (Rabassa 2008; Ramos and Ghiglione 2008). More recent events, mainly the Great Patagonian Glaciation (GPG; ca. 1 Mya), but also the Last Glacial Maximum (LGM; ca. 21 Kya), greatly altered the landscape of this region leaving an imprint on the distribution of genetic diversity in the Patagonian biota (Séršic et al. 2011). For instance, many Patagonian organisms show concordant intraspecific phylogeographic breaks following a latitudinal pattern (e.g. Lessa et al. 2010; Cosacov et al. 2010). Others share a pattern of decreasing genetic variability from east to west, suggesting that they survived Pleistocene glaciations in eastern Patagonia, and then migrated westwards during interglacial periods (reviewed in Séršic et al. 2011; but see Pfanzelt et al. 2017). Whether and how these lineage divergences resulted in niche divergence and in speciation is less clear.

A great opportunity to address this question is provided by sister species inhabiting continental Patagonia and the Malvinas/Falkland islands (Molau 1988; Sérsic and Cocucci 1996). These islands constitute the largest South Atlantic archipelago and are located at 52°S, lying close to the edge of the Patagonian continental shelf (~450 km from Tierra del Fuego; ~600 km east of mainland Argentina; Morrone and Posada 2005; McDowall 2005). Evidence suggests that these islands were colonized by Patagonian biota (i.e. Vuilleumier 1991; McDowall 2005; Papadopoulou et al. 2009; Bulgarella et al. 2013) either through long-distance dispersal or using land bridges appearing during Pleistocene glaciations, when western Patagonia was covered by the largest ice caps in South America and eastern Patagonia expanded around four longitudinal degrees to the east (Rabassa 2008; Ruzzante et al. 2008).

Unfortunately, the colonization history of the flora of the islands and its relationship with the Patagonian glacial records has been minimally investigated, and even less so from a phylogeographic perspective. A recent article give some support to the idea that the Malvinas/Falkland islands remained ice-free, being available for plant colonization when sea levels fell during glacial periods (Pfanzelt et al. 2017). To date, no plant studies have used explicit geo-statistical methods to explore the spatio-temporal dynamics of the connections between continental Patagonia and the Malvinas/Falkland islands.

The aim of this study is to reconstruct the biogeographic history of select Patagonian plants and determine if Quaternary climate-driven fluctuations affected the distribution of genetic diversity, lineage divergence, and speciation at the intra- and interspecific level. To do this, we disentangled the phylogeography of two sister species: *Calceolaria uniflora* Lam. (located in southern Patagonia and Tierra del Fuego; Fig. 1) and *C. fothergillii* Ait. (endemic to the Malvinas/Falkland islands; Fig. 1) using DNA sequences of one nuclear and two plastid loci, together with ecological data and niche modelling. The selected species provide an ideal study system because of their sister-species relationship, phenotypic similarity, low vagility, and allopatric distribution (Sérsic and Cocucci 1996; Cosacov et al. 2009). Based on the known biogeographic history of Patagonia and the Malvinas/Falkland islands, we hypothesize that the insular species originated from an ancestral population on continental Patagonia that colonized the islands during the lowest sea level glacial period (i.e. GPG) when a land bridge connecting mainland Patagonia with Malvinas/Falkland islands was formed. Following the post-glacial rise in sea level, geographic fragmentation and consequent population isolation could have resulted in differentiation of insular and continental populations via genetic drift (i.e. non-adaptive divergence). Alternatively, allopatric differentiation of the insular and continental lineages could have resulted from genetic drift, as well as niche differentiation (i.e. adaptive divergence) following glacial retreat and the subsequent exposure of the insular lineage to an oceanic climate. We expect that more recent glaciations occurring after GPG likely affected intraspecific patterns of distribution and demography of each species.

Under both scenarios (i.e. non-adaptive or adaptive divergence) we expect the divergence of this species pair began with the lack of gene flow after the GPG period. For the non-adaptive divergence scenario, we expect that the inferred paleo-distribution for the continental species will show suitable areas towards the exposed Patagonian shelf of the Atlantic coast and to the Falkland/Malvinas Islands during the glacial period, and a retraction of these suitable areas during interglacial periods. For the adaptive divergence scenario, we additionally expect to find significant differences between species when considering the background environmental differentiation.

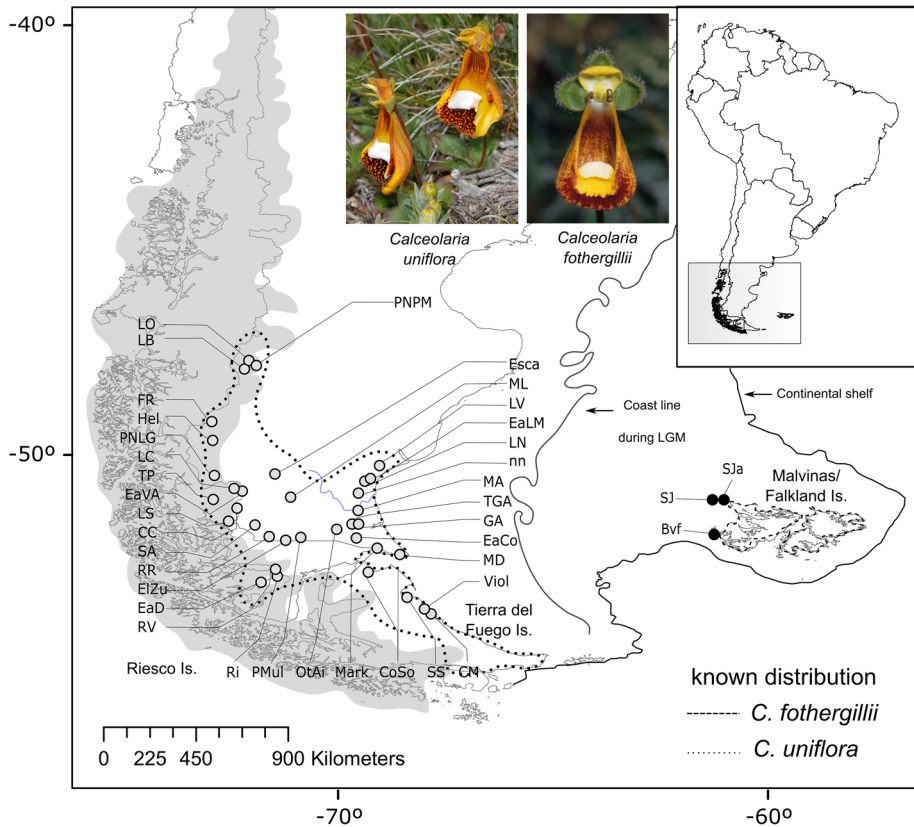


Fig. 1 Study area and sampling used in this study. Grey dots: *Calceolaria uniflora* localities. Black dots: *C. fothergillii* localities. Shaded area indicates extent of the ice cap during the Last Glacial Maximum (LGM) following Singer et al. (2004). The complete known distribution of each species is indicated with dashed lines. The black continuous line represents the continental shelf and the gray continuous line the position of coast line during LGM according to Ponce et al. (2011). The blue line represents the Coig River. See Supplementary material Table S1 for complete site names. Pictures depict both studied species (Photo of *C. fothergillii* courtesy of Dr. G. Gerlach). (Color figure online)

Materials and methods

Studied species

Calceolaria uniflora and *C. fothergillii* are among the few species of the New World genus *Calceolaria* that reach the high southern latitudes. *Calceolaria uniflora* occurs between 45° and 55°S in continental Patagonia, including Tierra del Fuego and southern associated islands (Fig. 1; Sérscic and Cocucci 1996; Ehrhart 2000), and grows in a variety of habitats. The species is found from the Atlantic coast and the Magellan Strait to an altitude of ~1200 m, occupying sub-Andean grasslands along the Andes, and the semi-arid Patagonian steppes. In contrast, *C. fothergillii* is a Malvinas/Falkland islands endemic and grows mainly on rocks, maritime cliffs and slopes, in coastal grasslands, and up to 174 m altitude (Upson et al. 2012). Unlike most *Calceolaria* species, which display oil-rewarding flowers and are pollinated by specialized oil-collecting bees

(Sérsic 2004), the two species studied here have modified floral oil-glands (elaiophores) that are white, fleshy and sweet (Fig. 1) and consumed by pollinating birds (Sérsic and Cocucci 1996; Sérsic 2004; Sérsic and Cocucci pers. obs.). Few phenotypic traits, such as floral colour patterns and plant pilosity, differentiate these species (Sérsic and Cocucci 1996). From a reproductive perspective, the species display low fruit and seed set by autogamy, relying on bird pollination for pollen transfer (Arroyo and Squeo 1990; Sérsic 2004; Mascó et al. 2004). Because seeds are dispersed mainly by gravity and wind (Molau 1988; Ehrhart 2000; Fernández et al. 2002), gene flow among populations via seeds is presumably limited.

Study area and sampling

Samples were collected from 38 localities (35 of *C. uniflora*; 3 of *C. fothergillii*), covering the range of both species. Geographic coordinates were recorded with a handheld GPS unit. Fresh leaves from one to 14 individuals per locality were collected for a total of 305 individuals (281 of *C. uniflora* and 24 of *C. fothergillii*; Fig. 1; Supplementary material Table S1). All collected individuals were at least 5 m apart from each other.

DNA extraction, amplification and sequencing

DNA material was extracted using a modified CTAB protocol (Doyle and Doyle 1987). Two chloroplast intergenic spacers *trnS-trnG* (primers *trnS*^[GCU] and *trnG*^[UCC]; Hamilton 1999) and *trnH-psbA* (primers *trnH*^[GUG] and *psbA*; Shaw et al. 2005) were sequenced. Chloroplast DNA (cpDNA) amplification consisted of 94 °C for 3 min followed by 30 cycles of 94 °C for 1 min, 52 °C for 1 min, and 72 °C for 1 min. We developed anonymous nuclear loci (ANL; Karl and Avise 1993) from a library of restriction digested genomic DNA of *C. polyrhiza*. Sequences were compared using BLAST to determine whether the locus showed significant BLAST hits, and screened for ANLs with levels of variability appropriate to this study. We choose one of these ANLs, CAL13, to survey across all individuals and populations, using primers CAL13F (5'-CTGACGGAGCATCAACAGAA-3') and CAL13R (5'-AAGGGATGAGGAAGA GAATGC-3') to amplify a region of approximately 500 bp. PCR amplification used a touch-down protocol consisting of 3 min at 95 °C followed by a total of 40 cycles of 94 °C for 30 s, variable annealing temperature for 30 s, and 72 °C for 45 s; the variable annealing temperature initiated at 62 °C, dropping one degree each cycle until 52 °C was reached, then continuing at 52 °C for the remaining 29 cycles. An additional 8 min at 72° was added following the 40 cycles.

Amplification products were purified using USB PrepEase PCR purification plates (Affymetrix Inc, Cleveland, OH, USA), sequenced with BigDye v.3 (Applied Biosystems, Foster City, CA, USA), and purified with Sephadex (GE Health-care, Piscataway, NJ, USA) before electrophoresis on an AB3730xl automated sequencer. Electropherograms were edited with ChromasPro v.1.7.7 and BioEdit v.7.0.9.0 (Hall 1999). Sequences were aligned with ClustalX v.1.81 (Thompson et al. 1997) using default parameters and adjusted by hand. Indels were coded as single binary characters using the simple indel coding method (Simmons and Ochoterena 2000). Two DNA matrices were constructed: one combining both cpDNA markers and the other with the nDNA sequences. Accessions representing all sequences were deposited in GenBank.

Haplotype/allele network, population genetic structure and genetic diversity

Haplotypes/alleles were inferred with DnaSP v.5 (Librado and Rozas 2009) for the concatenated *trnS-trnG/trnH-psbA* matrices. Individual alleles of nDNA heterozygotes were resolved with the coalescent-based Bayesian method PHASE v2.1 (Stephens et al. 2001), with the default settings. Genetic networks were inferred for both cpDNA and nDNA matrices using the median-joining algorithm implemented in Network v 5.0.0.1 (Bandelt et al. 1999).

cpDNA and nDNA haplotype/allele diversity (h ; Nei 1987), nucleotide diversity (π ; Nei 1987) and mean number of pairwise differences (p ; Tajima 1983) were calculated for each species, locality, and haplogroup observed in the network. To map genetic variation (h and π) on the geographic range of the species, we projected the haplotype/allele and nucleotide diversity values obtained at each of the 38 georeferenced localities into the modelled distribution of both plant species (see below) using the inverse distance weighting (IDW) spatial interpolation method (Watson 1992). For this, we used Quantum GIS 2.18 (Quantum GIS Development Team 2016).

To explore past historical barriers between groups of populations, we performed spatial analyses of molecular variance using SAMOVA v1.0 (Dupanloup et al. 2002). Analyses were run for K values ranging from K = 2–7, and using 10,000 independent annealing processes. We then selected the best clustering for each DNA type and for each K value using the among-group component (F_{CT}) of the overall genetic variance.

To explore the role of historical factors on the spatial genetic structure, we evaluated the potential influence of glacial extension (historical process) to explain nuclear and chloroplast genetic patterns. To test whether there were significant differences in the amount of genetic variation among refugia (i.e. non-glaciated regions) and recent colonized sites (i.e. glaciated regions) during the GPG, AMOVAs were performed separately for cpDNA and nDNA. Significance levels of variance components were computed using a nonparametric permutation approach with 10,000 replicates, implemented in Arlequin v3.11 (Excoffier et al. 2005).

Phylogenetic analyses and divergence time estimates

Because there are no known fossils of *Calceolaria*, we first reconstructed and calibrated a phylogeny based on Nylinder et al. (2012) to obtain the divergence time between *C. polyrhiza* and *C. uniflora*. This phylogeny included nuclear ITS sequences downloaded from GenBank of 11 phylogenetically distant *Calceolaria* species (according to Cosacov et al. 2009, including our species of interest), two representatives of the other Calceolariaceae genus, *Jovellana* (the South American *J. violaceae* and *J. punctata*), and *Kohleria spicata* (Gesneriaceae) as an outgroup external to the family (See Supplementary material Table S2; Fig. S1). After this analysis, we used a multispecies coalescent model to estimate the species tree based on multi-locus data under the Star BEAST (*BEAST; Heled and Drummond 2010) option implemented in BEAST v1.7.5 to reconstruct a calibrated coalescent relationships among *Calceolaria* populations using both cpDNA and nDNA complete data sets. This approach outperforms gene-concatenation methods in both species-tree topology inferences, and speciation-time estimations (Heled and Drummond 2010). For these analyses, we used three geographically distant individuals of *C. polyrhiza* as an outgroup (Supplementary material Table S3) and set as priors the time of divergence between *C. polyrhiza* and *C. uniflora* (2.73 ± 1.0 Ma) derived from the previous calibrated

analysis, and a chloroplast mutation rate (0.001–0.01 substitutions per site per million years; Alsos et al. 2005). The best-fit models of nucleotide substitution selected were HKY + I for the cpDNA matrix, and HKY + G + I for nDNA. Seven independent analyses were run for 3.0×10^8 generations, with a Yule tree prior, starting with a random tree and sampling parameters every 30,000 steps. We could confirm that only populations divergence parameters had high effective sample sizes ($ESS > 200$) using Tracer v1.6 (Rambaut and Drummond 2009). All the resulting topologies were visualized in DensiTree v2 (Bouckaert 2010), excluding the first 25% of the sampled trees. To obtain a more robust calibrations for the split between *C. uniflora* and *C. fothergillii* and their main lineages, we then reconstruct phylogenetic relationships among haplotypes/alleles and outgroups using our cpDNA nDNA data set separately in BEAST (Drummond et al. 2012). For these analyses, we used the same settings and priors mention above. We confirmed that the chains had reached stationarity and that parameters had high effective sample sizes ($ESS > 200$) using Tracer v1.6 (Rambaut and Drummond 2009). The maximum credibility tree was calculated using TreeAnnotator v1.7.5 (Rambaut and Drummond 2008), excluding the first 25% of the sampled trees (burn-in fraction of 0.25). At this point it is important to note, that although these estimates are provisional and should be interpreted with caution, they provide approximations that allow us to hypothesize possible scenarios under which lineages would have diverged.

Demographic history analyses

To assess the past demographic history of the genetic haplogroups observed in the haplotype network (*see results*), Tajima's *D* and Fu's *FS* (Tajima 1989; Fu 1997) tests were calculated for each dataset. Under sudden demographic expansion, both indices show significant negative values and the null hypothesis of long-term mutation-drift balance is rejected. Significance was calculated from 1000 simulated samples using a coalescent process. Along with these two tests, we also used the mismatch distribution of pairwise differences among individuals. Here, populations at demographic equilibrium are expected to show a multimodal distribution, whereas populations having experienced recent demographic expansion typically show a unimodal distribution (Excoffier 2004). Goodness of fit of the observed mismatch distribution to that expected under a sudden expansion model was evaluated with the sum of squared deviations (SSD) using parametric bootstrapping (10,000 replicates). Analyses were performed in DnaSP v5 and Arlequin 3.11 (Excoffier et al. 2005).

We also determined the shape of the population growth (*N_e*) curve through time using Extended Bayesian Skyline Plots (EBSP; Heled and Drummond 2008) implemented in BEAST v2.4.8 for the genetic groups observed in *BEAST analysis, using the cpDNA and nDNA dataset with coalescent tree prior specified as extended Bayesian skyline. This approach allows estimation of population size changes over time and improves the reliability of demographic inferences because of its power in detecting past population change increases, and substantially reducing the estimation error given the multilocus framework. For these analyses, we used the HKY model for all datasets (*see results*) according to the Akaike criteria (AIC), as implemented in JmodelTest. Two MCMC starting with a random tree were run for 1×10^7 generations, with parameters sampled every 10,000 steps. For this analysis we used the mutation rate of nDNA derived from the dated genealogy (estimated between 0.0065 and 0.0022 substitutions per site per million years) and the same mutation rate of cpDNA used in our previous analysis (0.001–0.01 substitutions per site per million years; Alsos et al. 2005). Chain convergence check and burn-in were the same

as previously described for the *BEAST reconstruction. Posterior distributions generated from the EBSF analyses were used to construct plots with the plotEBSF function provided by BEAST version 2.3.2 (<https://www.beast2.org/tutorials/>) in R version 3.2.3, containing the median and central posterior density of the effective population size and the time to the most recent common ancestor.

Bayesian spatio-temporal diffusion analyses

To explore whether demographic expansion was coupled with a process of range expansion we reconstructed the evolutionary history of lineages through time in BEAST assuming for continuous spatial diffusion using a time-heterogeneous random walk model (“Relaxed Random Walk”, RRW, Lemey et al. 2010). This Bayesian approach to infer ancestral distribution of lineages through time and space has only recently been applied to the study of diffusion dynamics of organisms with relatively slower evolutionary rates (Nascimento et al. 2013; Werneck et al. 2015; Baranzelli et al. 2017; Kébé et al. 2017). Independent analyses were run for cpDNA and nDNA datasets, with each dataset including one sequence per haplotype/allele represented at each site (e.g. Camargo et al. 2013; Bielejec et al. 2016; Baranzelli et al. 2017). For each analysis, we used a normally distributed diffusion rate, a coalescent Bayesian Skyride model, and GTR and GTR+I+G substitution models for cpDNA and nDNA, respectively. The corresponding mutation rate for each data set, the divergence time between *C. uniflora* and *C. fothergillii* lineages (see *results*) for the cpDNA dataset, and the root divergence time of the ingroup for the nDNA dataset were used as temporal informative priors. The remaining parameters, clock model, chain convergence and tree annotation were the same as for the previous bayesian analyses. We used the *jitter* option on statistical TraitLikelihood with a parameter of 0.01 at add variation to sequences with the same geographic location. For each marker type, we performed two independent runs of 100 million generations sampled every 10,000 generations, to obtain a total of 10,000 trees from the posterior distribution. We combined both resulting *log* and *tree* files, and inspected parameter traces with Tracer to check for stationarity. To summarize the posterior distribution of ancestral ranges using the RRW model, we annotated nodes in a maximum clade credibility tree (MCC) using the program TreeAnnotator v1.7.5. This tree was then used as an input in SPREAD v1.0.7 (Bielejec et al. 2011). to reconstruct the pattern of spatial diffusion (e.g. Camargo et al. 2013).

Paleo-distribution models

Species distribution models under different past climatic scenarios were analyzed for both *Calceolaria* species. We used 61 georeferenced *C. uniflora* from the field, but also from herbarium records (CORD, IS, Herbario del Instituto de la Patagonia-Chile, and CONC), and 49 georeferenced *C. fothergillii*, obtained from Falklands Conservation (Supplementary material Table S4). From these georeferenced locations, current climatic data with grid cell resolution of 0.25 degrees (~5 km² cell), were downloaded from the WorldClim database v1.4 (<http://www.worldclim.org/>; Hijmans et al. 2005); following Braunisch et al. (2013) we used all 19 bioclimatic variables derived from the monthly temperature and rainfall values. All bioclimatic layers were cropped to span from 43.86°S to 56.51°S and from 75.52°W to 55.44°W, a spatial range that contains the current ranges of *C. uniflora* and *C. fothergillii*.

We estimated the species distribution model using the current bioclim variables using the Maximum Entropy algorithm in MaxEnt v3.3.3 (Phillips et al. 2006) and DIVA-GIS v7.5 (Hijmans et al. 2005). MaxEnt was run using the following settings: random test percentage = 25; convergence threshold = 0.00001; maximum iterations = 1000 and averaged across 10 bootstrap runs. In addition, we selected the autofeatures option in MaxEnt to describe relationships between specimen locations and environmental conditions. Moreover, given the restricted distribution of both species, we selected a value of regularization multiplier = 0.75 instead of the default value, to avoid over dispersion of the projected models outside the current distribution range known for the species (Anderson and Gonzales 2011). We used the lowest value of probability of occurrence, obtained among the trustable points of presence used in the model for each species, as the threshold value for each prediction. Finally, a jackknife test was conducted to assess the relative importance to the model of each environmental variable included. To measure model fit, we used the partial area under the receiver operating curve (pROC; Peterson et al. 2008) in “Partial ROC” software (Barve 2008). We used 10,000 iterations, and for each iteration, we re-sampled 50% of the test data and accepted a 95% of error (default settings). Here, a partial AUC ratio > 1 for the model indicates that performance is better than random. Partial ROC is better than conventional ROC, among other reasons, because the Area Under Curve calculation is restricted to the domain of prediction of the algorithm, and do not extend to intervals where did not make predictions thus, overestimating the specificity of the model (Peterson et al. 2008).

To estimate how species distributions may have changed through time, this model was projected for each of the palaeoclimatic scenarios, from the mid-Pliocene (PLI; 3.3–3.0 Mya; Lima-Ribeiro et al. 2015), the Last Interglacial period (LIG; 130–114 Kya; Otto-Bliesner et al. 2006), the LGM (21 Kya) and the mid Holocene (6 Kya), based on the Community Climate System Model (CCSM4). For the last two periods, we also evaluated the simulation based on the Model for Interdisciplinary Research on Climate (MIROC-ESM), and the predicted presence probabilities obtained with CCSM and MIROC were averaged to obtain a combined result.

Climatic niche differentiation

We tested for climatic niche differentiation between *C. uniflora* and *C. fothergillii* taking into account the fact that species currently have different available habitats in a spatially autocorrelated landscape (McCormack et al. 2009). Ten of the 19 environmental variables were chosen to test for differences among the allospecies based on their biological relevance (Annual Mean Temperature (AT), Annual Precipitation (AP), Mean Temperature and precipitations of Warmest (TWaS and PWaS), coldest (TCS and PCS), driest (TDS and PDS) and wettest (TWeS and PWeS) season. Most of these variables were retrieved as important by MaxEnt in the PDM (see *Results*).

The climatic data from occurrence points, plus 1000 random background points taken from the geographic range of each species were reduced with principal components analysis (PCA) to three axes explaining almost all variance (96%). Then, to examine niche divergence or conservatism between the *Calceolaria* species, across each of these three niche axes, we tested against a null model of background divergence by comparing the observed difference in mean niche values (species niche distance; SND) to the difference in mean background values (species background distance; SBD) following McCormack et al. (2009). Significance was assessed with 1000 jack-knife replicates of the mean background

values. All analyses were performed in R v.3.3.2 using the ‘car’ and ‘boot’ packages. The scripts used is provided as supplemental material (Supplementary material Table S5).

Results

DNA sequence matrices

A total of 305 individuals were sequenced for the cpDNA. The intergenic spacers *trnS-trnG* and *trnH-psbA* included 740, and 260 bp, respectively. As the chloroplast is typically inherited uni-parentally without recombination, these two regions were combined into a single matrix (1000 bp), providing 37 polymorphic sites (3.7%). We sequenced 193 individuals at the nuclear anonymous region (CAL13); this alignment was 471 bp of which 21 were variable sites (4.45%). The aligned databases were deposited in TreeBase.

Haplotype/allele network, population genetic structure, and genetic diversity

The haplotype network reveals a clear geographic structure for the cpDNA lineages. The insular species *C. fothergillii* was retrieved in a distinct group with H1, H2, H22 and H23 as exclusive haplotypes separated from *C. uniflora*'s haplotypes by nine to 15 mutational steps (Fig. 2a). Within *C. uniflora*, three main haplogroups were distinguished: a western group (West) containing the most frequent haplotypes H3 (33.11%), and two eastern steppe groups, a northern group (Steppe North) containing H7 and H8 and their derivatives, and a southern group (Steppe South) represented by H6 and derivatives. Both steppe haplogroups reached Tierra del Fuego (Fig. 2a). Haplotype richness per site ranged from one to five; a total of 16 sites were monomorphic most of them for H3 to the West, and for H6 to the South, while the steppe site OtAi had the highest haplotype richness (five haplotypes; Table 1).

The 18 alleles retrieved in the nDNA data set show less geographic structure compared to the chloroplast markers (Fig. 2b). Among the alleles, nH3 (41.62%), nH1 (23.92%) and nH9 (8.61%) were the most frequent. Allele nH1, mostly distributed in the western part of the range of *C. uniflora*, was also the only allele in the Malvinas/Falkland islands. *Calceolaria uniflora* showed two well-defined western haplogroups in the network with overlapping at geographical scale; one formed by nH5–7 and their derivatives (West 1), and the other by nH1 and nH9 and derivatives (West 2; Fig. 2b). The last haplogroup observed in the network was formed only by nH3, which is separated from the remaining alleles by 11 mutational steps and is mainly distributed along the steppe (Steppe; Fig. 2b). Allele richness per site ranged from one to nine; 11 sites were monomorphic, most of them towards the East harboring nH3 (Table 1). The highest allele richness was found in western localities, with Helsingfors being the site with highest allelic richness. Geographic distribution of heterozygosity showed a clear east–west pattern, with a higher proportion of heterozygous individuals at the western area of the distribution range (Supplementary material Fig. S2).

The geographic interpolation of genetic diversity (h and π) showed high nucleotide diversity distributed around 52°S latitude for both loci (Fig. 3a, b). In contrast, haplotype/allele diversity of the two loci showed opposite spatial distribution patterns: while cpDNA

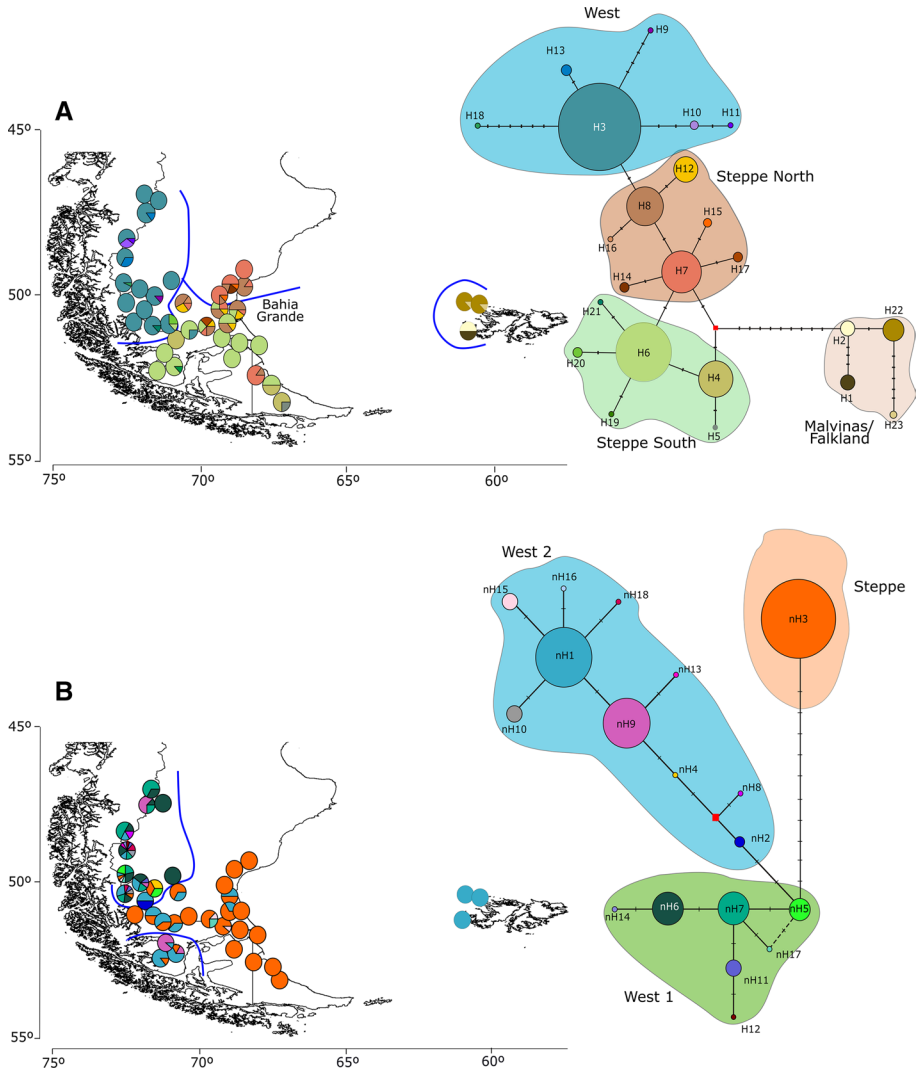


Fig. 2 Spatial distribution (left) and haplotype network (right) reconstructed for *Calceolaria uniflora* and *C. fothergillii*. **a** cpDNA. **b** nDNA. On the maps, portions of pie charts represent the frequency of occurrence of each haplotype/allele in each population. Haplotype/allele colours correspond to those shown in the networks. Blue lines in the map correspond to the main genetic groups retrieved by SAMOVA. In the networks, colored areas correspond to the genealogical groups, haplotypes/alleles are designated by numbers; circle sizes proportional to haplotype/allele frequencies. Segments between dashes indicate mutational steps; red dots represent missing intermediate haplotypes/alleles not observed in the analyzed individuals. (Color figure online)

haplotype diversity was most diverse in the eastern and southern areas of the species ranges (Fig. 3c), nDNA allele diversity was highest in the westernmost areas (Fig. 3d).

The SAMOVA structure analysis performed on the cpDNA matrix showed an optimal partition of genetic diversity of $K=3$ ($F_{CT}=0.80$, $P<0.0001$), revealing three genetic groups located in the Malvinas/Falkland Islands, along the steppe and along the Andean

Table 1 Diversity indices and results of demographic analyses in *Calceolaria uniflora* and *C. foeterrigillii* populations for cpDNA and rDNA. Names of localities, ample size (#ind), polymorphic sites (S), haplotypes/alleles (H), haplotype/allele diversity (h), nucleotide diversity (π), and mean number of pairwise differences (\bar{p}) are shown

Chloroplast DNA										Nuclear DNA				
Site	#ind	S	H	h (\pm SD)	π (\pm SD)	\bar{p} (\pm SD)	#ind	S	H	h (\pm SD)	π (\pm SD)	\bar{p} (\pm SD)		
BvIf	8	4	H1, H2	0.5714 (0.0945)	0.0021 (0.0016)	2.28571 (1.3976)	1	0	H1	0.0000	0.0000	0.0000		
CC	8	0	H3	0.0000	0.0000	0.0000	4	6	H1, H2	0.6667 (0.2041)	0.0085 (0.0064)	4.0000 (2.5175)		
CMu	4	1	H4, H5	0.5000 (0.2652)	0.0005 (0.0006)	0.5000 (0.5191)	4	0	H3	0.0000	0.0000	0.0000		
CoSo	4	0	H6	0.0000	0.0000	0.0000	5	0	H3	0.0000	0.0000	0.0000		
EaCo	8	0	H6	0.0000	0.0000	0.0000	4	0	H3	0.0000	0.0000	0.0000		
EaD	8	0	H6	0.0000	0.0000	0.0000	7	18	H1, H3	0.2857 (0.11964)	0.0109 (0.0070)	5.1428 (2.8345)		
EaLM	7	1	H7, H8	0.2857 (0.1964)	0.0003 (0.0004)	0.2857 (0.3409)	2	0	H3	0.0000	0.0000	0.0000		
EaVa	8	4	H3, H9	0.2500 (0.1802)	0.0010 (0.0008)	1.0000 (0.7489)	2	16	H3, H4, H5	1.0000 (0.2722)	0.0226 (0.0178)	10.6667 (6.7236)		
EIZu	14	0	H4	0.0000	0.0000	0.0000	5	18	H1, H3	0.5357 (0.1232)	0.0205 (0.012)	9.6428 (4.9509)		
Esca	9	0	H3	0.0000	0.0000	0.0000	6	12	H3, H6	0.5333 (0.1721)	0.0136 (0.0087)	6.4000 (3.5327)		
FR	10	3	H3, H10, H11	0.6000 (0.1305)	0.0013 (0.0016)	1.2667 (0.8680)	6	10	H1, H6, H7, H8	0.8000 (0.1721)	0.0092 (0.0061)	4.3333 (2.4922)		
GA	10	2	H6, H7, H8, H12	0.7333 (0.1199)	0.0010 (0.0008)	1.0000 (0.7326)	4	0	H3	0.0000	0.0000	0.0000		
Hel	9	1	H3, H13	0.5000 (0.1283)	0.0005 (0.0005)	0.5000 (0.4665)	9	10	H1, H6, H7, H9, H10, H11, H12, H13, H14	0.9333 (0.0397)	0.0112 (0.0064)	5.2571 (2.6919)		

Table 1 (continued)

Chloroplast DNA										Nuclear DNA				
Site	#ind	S	H	h (±SD)	π (±SD)	p (±SD)	#ind	S	H	h (±SD)	π (±SD)	p (±SD)		
LB	7	1	H3, H13	0.2857 (0.1964)	0.0003 (0.0004)	0.2857 (0.3409)	6	9	H6, H7, H9	0.6071 (0.1640)	0.0096 (0.0060)	4.5357 (2.4933)		
LC	8	0	H3	0.0000	0.0000	0.0000	7	10	H1, H6, H7, H9, H11	0.8444 (0.0796)	0.0112 (0.0067)	5.2667 (2.7800)		
LN	10	3	H7, H8, H14, H15	0.7333 (0.1199)	0.0009 (0.0008)	0.0009 (0.0008)	-	-	-	-	-	-		
LO	8	0	H3	0.0000	0.0000	0.0000	3	1	H6, H7	0.6667 (0.3143)	0.0014 (0.0018)	0.6667 (0.6667)		
LS	8	0	H3	0.0000	0.0000	0.0000	4	0	H3	0.0000	0.0000	0.0000		
LV	7	3	H7, H8, H12, H16	0.8095 (0.1298)	0.0010 (0.0009)	1.0476 (0.7848)	6	18	H1, H3	0.5333 (0.1721)	0.0204 (0.0126)	9.6000 (5.1381)		
MA	8	2	H6, H7, H8, H12	0.8214 (0.1007)	0.0011 (0.0009)	1.1071 (0.8042)	4	14	H1, H3	0.6667 (0.2041)	0.0255 (0.0175)	12.0000 (6.9057)		
Mark	8	0	H6	0.0000	0.0000	0.0000	9	17	H3, H15	0.2222 (0.1662)	0.0080 (0.0051)	3.7778 (2.0990)		
MD	7	0	H6	0.0000	0.0000	0.0000	6	0	H3	0.0000	0.0000	0.0000		
ML	5	0	H7	0.0000	0.0000	0.0000	8	0	H3	0.0000	0.0000	0.0000		
nn	8	2	H7, H8, H15	0.4643 (0.2000)	0.0005 (0.0005)	0.5000 (0.4717)	1	0	H3	0.0000	0.0000	0.0000		
OrAi	8	3	H6, H7, H8, H12, H17	0.8929 (0.0858)	0.0015 (0.0011)	1.5000 (1.0057)	7	19	H3, H15, H16	0.5238 (0.2086)	0.0184 (0.0111)	8.6667 (4.5612)		
PMul	8	4	H3, H6	0.4286 (0.1687)	0.0017 (0.0013)	1.7143 (1.1136)	2	0	H3	0.0000	0.0000	0.0000		
PNLG	8	6	H3, H18	0.1333 (0.1123)	0.0008 (0.0007)	0.8000 (0.6110)	7	20	H1, H3, H5, H6, H7, H15, H17	0.8571 (0.0573)	0.2004 (0.1182)	4.2095 (2.2136)		

Table 1 (continued)

Chloroplast DNA										Nuclear DNA				
Site	#ind	S	H	h (±SD)	π (±SD)	p (±SD)	#ind	S	H	h (±SD)	π (±SD)	p (±SD)		
PNPM	5	0	H3	0.0000	0.0000	0.0000	4	0	H6	0.0000	0.0000	0.0000		
Ri	8	1	H6, H19	0.2500 (0.1802)	0.0002 (0.0004)	0.2500 (0.3113)	6	18	H1, H3, H9	0.6000 (0.2152)	0.0132 (0.0084)	6.2000 (3.4322)		
RR	7	5	H3, H6, H20	0.6667 (0.1598)	0.0028 (0.0019)	2.7619 (1.6584)	5	18	H1, H3	0.6000 (0.1753)	0.0229 (0.0147)	10.8000 (5.9367)		
RV	8	0	H6	0.0000	0.0000	0.0000	9	1	H1, H9	0.3889 (0.1644)	0.0008 (0.0010)	0.3889 (0.3995)		
SA	8	5	H3, H21	0.2500 (0.1802)	0.0013 (0.0010)	1.2500 (0.8782)	2	18	H1, H3	1.0000 (0.5000)	0.0382 (0.0393)	18.0000 (13.0767)		
SJ	8	5	H22, H23	0.2500 (0.1802)	0.0013 (0.0010)	1.2500 (0.8782)	7	0	H1	0.0000	0.0000	0.0000		
SJa	8	5	H22, H23	0.2500 (0.1802)	0.0013 (0.0010)	1.2500 (0.8782)	4	0	H1	0.0000	0.0000	0.0000		
SS	7	1	H7, H8	0.2857 (0.1964)	0.0003 (0.0004)	0.2857 (0.3409)	7	18	H1, H3, H9	0.6667 (0.11598)	0.0212 (0.0127)	10.0000 (5.2132)		
TGA	14	2	H6, H8, H12	0.6484 (0.0813)	0.0010 (0.0008)	1.0330 (0.7318)	3	18	H1, H3	0.6667 (0.3143)	0.0255 (0.0199)	12.0000 (7.52149)		
TP	9	0	H3	0.0000	0.0000	0.0000	11	20	H1, H3, H6, H7, H10, H12, H18	0.9091 (0.0656)	0.0151 (0.0087)	7.1273 (3.6229)		
Viol	8	1	H4, H6	0.5714 (0.0945)	0.0006 (0.0006)	0.5714 (0.5134)	6	0	H3	0.0000	0.0000	0.0000		

Sites in bold correspond to *C. foftergillii*

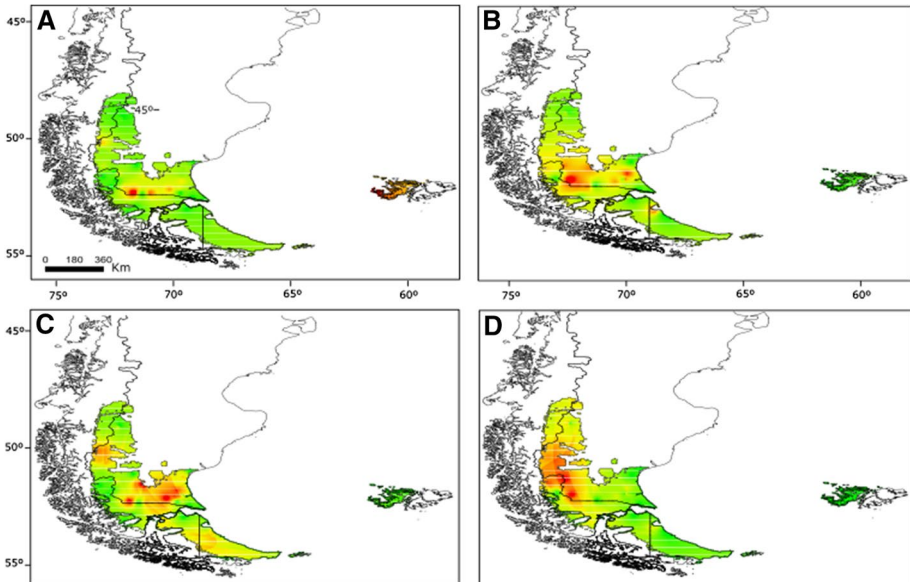


Fig. 3 Inverse distance weighting (IDW) spatial interpolation of nucleotide (π) and haplotype/allele (h) genetic diversity for cpDNA haplotypes (a, c, respectively) and for nDNA alleles (b, d, respectively). Red colors indicate highest and green colors the lowest molecular diversity. (Color figure online)

slopes to the West. A second independent analysis was run only with the steppe group retrieving a southern and a northern partition that correspond to the haplogroups recovered in the haplotype networks (Fig. 2a). The nDNA dataset, in turn, showed that five groups ($K=5$) was the most optimal partition of the genetic diversity ($F_{CT}=0.58$, $P<0.0001$). We found a western group mostly coincident with the cpDNA western group, a group mostly distributed along the steppe containing the monomorphic localities for nH3, a third cluster containing localities with alleles of divergent lineages containing nH1 and nH3, a small fourth group which includes only localities of the Riesco island and including also alleles of different lineages (nH3 and nH1), and a fifth group containing all monomorphic *C. fothergillii* populations. Therefore, for the nDNA demographic analyses, we followed the groupings in the haplotype network (Fig. 2b).

Finally, results of the AMOVA performed to test differences of genetic diversity among populations located in areas covered versus uncovered by ice during the GPG showed a significant difference only in cpDNA, showing in unglaciated populations more genetic diversity than in glaciated ones (Table 2).

Phylogenetic analyses and divergence time estimates

The calibrated ITS phylogeny retrieved *Calceolaria uniflora* and *C. fothergillii* in a well-supported monophyletic clade that would have diverged from *C. polyrhiza* around 3 Mya (95% Highest Posterior Density, HPD=2.12–4.37Mya; Fig. 4a, c). The Bayesian multi-locus dated genealogy retrieved the two focal species as reciprocally monophyletic with a moderate support (PP=0.83–0.94) and estimated the mean of populations divergences at around 0.16 ± 0.07 Mya (Fig. 4a, b). Unilocus calibrated trees, dated the most recent common ancestor of *C. fothergillii* and *C. uniflora* at around 1.2 Mya (95%

Table 2 Results of the analysis of molecular variance (AMOVA) for 38 populations for cpDNA and 37 for nDNA to test association of genetic diversity among populations located in areas covered versus uncovered by ice during the Great Patagonian Glaciation. Degrees of freedom (d.f.). Sum of squares (SSD). Variance components (VC)

	Source of variation	d.f.	SSD	VC % Total	P value
cpDNA	Glaciated versus non-glaciated	1	78.303	0.489	< 0.001
	Among populations	36	403.86	1.364	< 0.001
	Within populations	267	82.139	0.307	< 0.001
	Total	304	564.302	2.161	
nDNA	Glaciated vs. non-glaciated	1	20.151	0.056	0.275
	Among populations	35	528.259	2.281	< 0.001
	Within populations	172	400.623	2.329	< 0.001
	Total	208	949.033	4.666	

Percentage of total variance (% total) and significance value (*P*) are given for each hierarchical level

HPD=0.71–2.00 Mya), dating the diversification within *C. fothergillii* at around 470 Kya (95% HPD=0.19–0.83 Mya), while within *C. uniflora* the moderate supported steparian and western clades (PP=0.67 and 0.80, respectively), which are in concordance with the western and eastern groups retrieved by SAMOVA, would have diverged at around 680 Kya (95% HPD=0.38–1.11 Mya; Fig. 4a and Supplementary material Fig.S3).

Demographic history

Almost no signals of demographic expansion was retrieved for *C. fothergillii* (Table 3), while for *C. uniflora* demographic analyses showed clear evidence of demographic expansion for the western lineages of both cpDNA and nDNA as indicated by the negative and significant values of Fu's and/or Tajima's neutrality tests, and by the non-significant result of the mismatch distribution analysis. The Steppe South haplogroup of the cpDNA showed a weaker signal of sudden demographic expansion (Table 3).

The EBSP results performed for *C. fothergillii* showed a slightly population increase between 150 and 80 Kya, after that time it stabilizes (Fig. 4d, top); EBSP inferences for the *Calceolaria uniflora* western lineages showed a constant effective population size until the present (Fig. 4d, centre), while the steparian lineages retrieved a recent demographic increase up to the present, starting at 40 Kya (Fig. 4d, bottom).

Bayesian spatio-temporal diffusion analyses

Both RRW diffusion models showed the ancestral geographic area of the species located around 50°–51°S. However, in the cpDNA, the ancestral area was inferred in the eastern coast, at 69°W (Fig. 5a; sites EaLM, MA, Mark, TGA), while the nDNA dataset recovered the ancestral population in the central Patagonian steppe, at 71°W (LV, Esca; Fig. 5e).

The cpDNA spatio-temporal diffusion indicates that a first expansion started around 800 Kya (Fig. 5a). From this area, two lineages started colonizing the west of the steppe (LV, Esca) and the Malvinas/Falkland islands. At around 580 Kya the lineage leading to *C. fothergillii* arrived to the islands, while *C. uniflora* colonized four new mainland areas from the ancestral region (Fig. 5b). At about 350 Kya, one *C. uniflora* lineage dispersed to Tierra

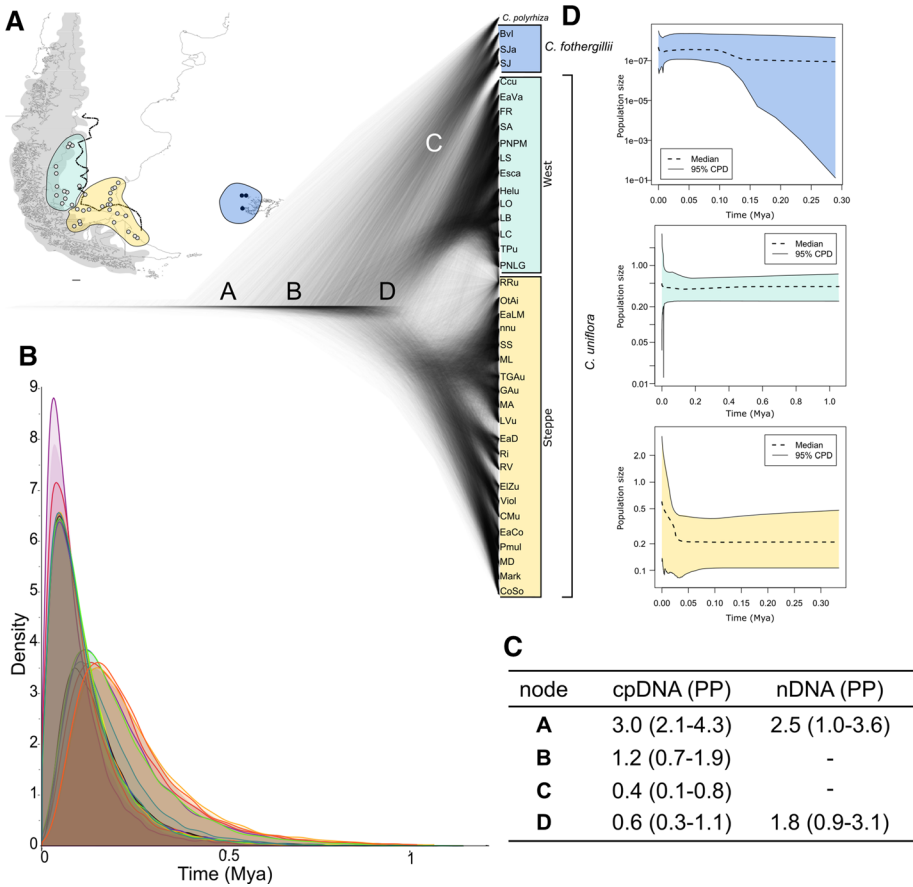


Fig. 4 **a** Visualisation of all the sampled multilocus coalescent trees reconstructed based on cpDNA and nDNA sequences. Vertical colored boxes on the right indicate clusters containing the outgroup and ingroup species; the map to the left shows the geographical distribution of *C. fothingillii* and *C. uniflora* main lineages. Letters given for each node are in correspondence with pannell C. **b** Posterior density plots of divergence times for each population of *C. fothingillii* and *C. uniflora*. **c** Divergence times in million years estimated for each supported node (PP>0.67) showed in pannell A. **d** Extended Bayesian skyline plot (EBSP) showing changes in effective population size [Ne; median ± 95% central posterior density (CPD)] over time for the three main clades observed in **a**. (Color figure online)

del Fuego, reaching the full extent of the current species range; the last range expansions occurred around 120 Kya into the southernmost areas of Tierra del Fuego, and to the northernmost sampled sites in PNPm (Fig. 5c, d). Since the LIG (120 Kya) and during the LGM (21 Kya), both species diversified locally without expanding its range.

The nDNA dataset showed that the ancestral lineages originated at about 1.25 Mya (Fig. 5e). From this ancestral area and at about 800 Kya the differentiation of the shared haplotype between *C. uniflora*–*C. fothingillii* (nH1) started (Fig. 5f), with the lineage arriving to the Malvinas/Falkland islands around 580 Mya (Fig. 5g). Within *C. uniflora*, two main regions were established from the beginning of the dispersal from the ancestral area: one at the west and the other at the east, which were interconnected twice between 900 and

Table 3 Number of individuals, number of haplotypes/alleles (K), genetic (h , π , p), and demographic indices (D, F_s , and SSD) obtained for the groups identified according to genealogical relationships within cpDNA and nDNA

Groups	#ind	K	h (\pm SD)	n (\pm SD)	p (\pm SD)	Demographic analyses			Species
						D	F_s	SSD	
cpDNA									
Malvinas/Falkland	24	4	0.6232 (0.0907)	0.0024 (0.0015)	2.4203 (1.3600)	-0.32094	2.753	0.1025	<i>C. fothergillii</i>
Steppe North	71	7	0.6833 (0.0327)	0.0009 (0.0007)	0.9038 (0.6358)	-0.6477	-1.9108	0.0171***	<i>C. uniflora</i>
Steppe South	100	6	0.4117 (0.0507)	0.0004 (0.0004)	0.4462 (0.4006)	-1.1453	-2.9574	0.0069	
West	110	6	0.1561 (0.0466)	0.0003 (0.0003)	0.3030 (0.3175)	-1.9137***	-2.8319*	0.0045	
nDNA									
Steppe	87	1	0.00 (0.00)	0.00 (0.00)	0.00 (0.00)	-	-	-	<i>C. uniflora/C. fothergillii</i>
West 1	48	7	0.6853 (0.0435)	0.0020 (0.0015)	0.9778 (0.6751)	-0.3228	-2.11326	0.0122	
West 2	81	10	0.5725 (0.0537)	0.0020 (0.0015)	0.9598 (0.6618)	-1.2124	-4.6045*	0.0088	

Values in bold indicate signals of demographic expansion

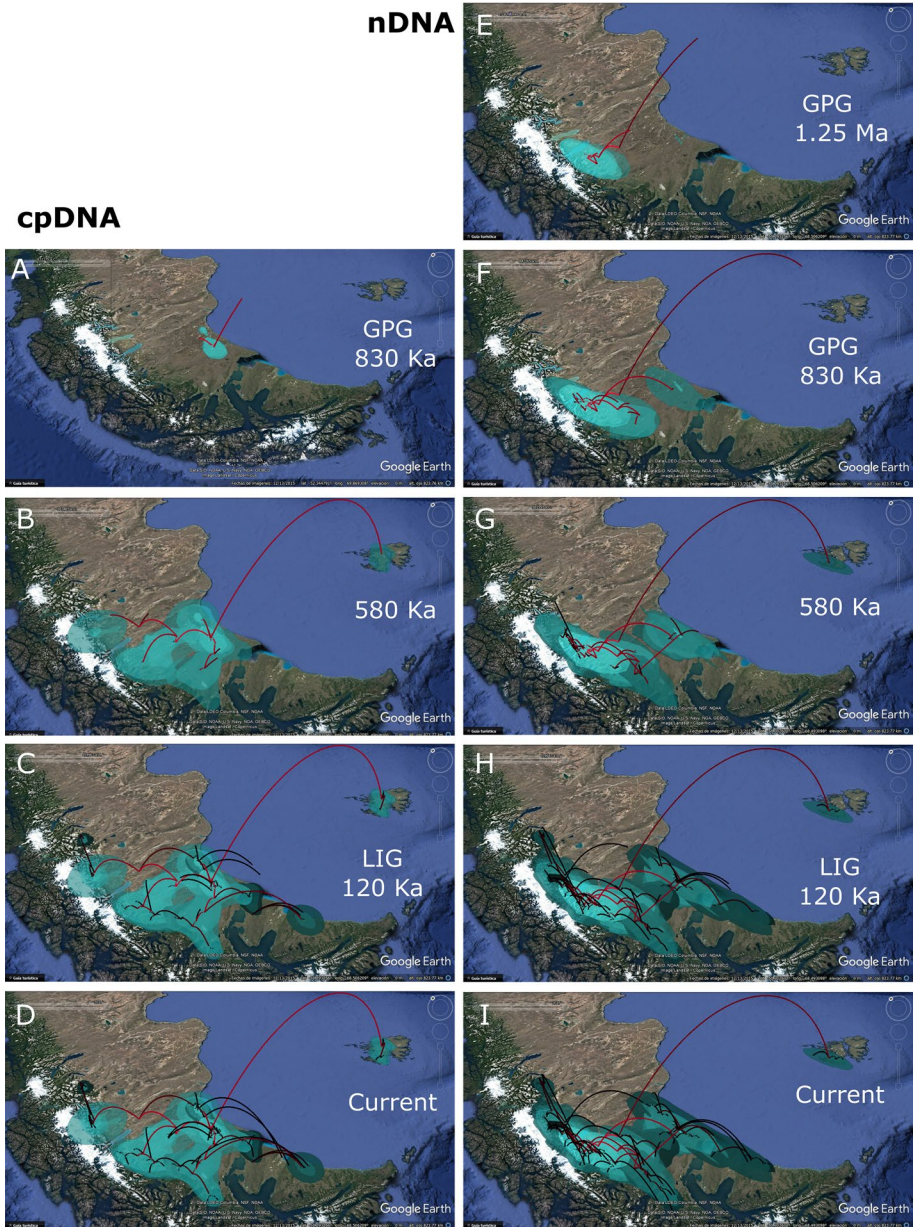


Fig. 5 Bayesian spatio-temporal diffusion analysis of *Calceolaria uniflora* and *C. fothergillii* cpDNA (a–d) and nDNA (e–i) lineages at different time points, and based on the maximum clade credibility (MCC) tree. Time slices are: 1.25 Ma (GPG; only nDNA), 830, 580, 120 Ka and present time. Lines represent branches of the MCC tree; shaded areas: 80%-HPD uncertainty in the location of ancestral branches, shading gradient indicates older versus younger events

800 Mya. From around 600 Kya and up to the present, several diversifications and range expansions to multiple directions occurred in *C. uniflora* (Fig. 5h, i).

The mean spatial diffusion rate for the cpDNA was 343 km/Ma (=0.34 m/year; 95% HPD: 0.04–1), and for the nDNA was 210 km/Ma (=0.21 m/year; 95% HPD: 0.09–0.35). (Supplementary material Video V1 and V2, respectively).

Paleo-distribution

With respect to the species distribution models, the pROC average value obtained for *C. uniflora* for current climatic conditions after ten runs was 1.995 ± 0.002 , and the threshold value selected was 0.311 ± 0.020 . The variables that contributed most to the current models for *C. uniflora* and for *C. fothergillii* are summarized in the Supplementary material, Tables S6 a,b. For *C. fothergillii* the pROC average value was 1.923 ± 0.007 and the threshold value selected was 0.207 ± 0.058 . The paleo-distribution reconstructed for the mid-Pliocene (3–3.3 Mya) suggests great similarity in the climatic suitability of both species around the Atlantic coast (Fig. 6a). For *C. uniflora*, the most suitable areas were in the southwestern portion of the range, while for *C. fothergillii*, they were restricted to a small coastal portion in the north of Tierra del Fuego. During the LIG (120 Kya), the paleo-distribution models (PDMs) suggest a drastic reduction in the suitable area for *C. uniflora*, with it being mainly restricted to the foothills of the Andes, along a latitudinal strip (Fig. 6b). For *C. fothergillii*, suitable conditions disappear in the mainland and are restricted to the easternmost portion of the Malvinas/Falkland islands. The distribution models for the LGM (Fig. 6c) suggest that this glaciation period could have favoured the expansion of both species. In *C. uniflora*, an eastward shift is evident towards the exposed Patagonian shelf of the Atlantic coast and the Falkland/Malvinas Islands. High suitabilities for *C. fothergillii* shifted towards the north and west of the Malvinas/Falkland islands. During the middle Holocene, 6 Kya, our projections identify a retraction of suitable areas for both species, more drastic in *C. fothergillii* than in *C. uniflora* (Fig. 6d). The projections onto current climatic conditions showed areas with high probability of occurrence across the entire southern Patagonia for *C. uniflora*, and the Malvinas/Falkland islands for *C. fothergillii* (Fig. 6e). These models suggest a progressive increment of climatically favourable areas for *C. fothergillii* from the LGM to the present. In contrast, in *C. uniflora*, the favourable areas continued to decrease in size and finally become fragmented (Fig. 6e).

Climatic niche differentiation

Species occurs in regions with similar mean annual temperature conditions ($6.05 (\pm 0.8) ^\circ\text{C}$ for *C. uniflora* and $6.09 (\pm 0.3) ^\circ\text{C}$ for *C. fothergillii*), but different mean annual precipitations ($314 (\pm 138)$ mm for *C. uniflora*, and $550 (\pm 37)$ mm for *C. fothergillii*). The climatic PCA clearly separated both species in space (Fig. 7a). PC1 explained most of the variation through five precipitation variables (64%); PC2 explained 17% of the variation, characterized mainly by temperature variables (AT, TCS); PC3 explained 15% and was mostly correlated with temperature of the driest and wettest quarters. *Calceolaria uniflora* appeared scattered in the climatic space, though more associated with drier and colder conditions than *C. fothergillii*. Compared to null models of background divergence, PC1 showed evidence for niche divergence, while PC2 showed significant evidence for niche conservatism,

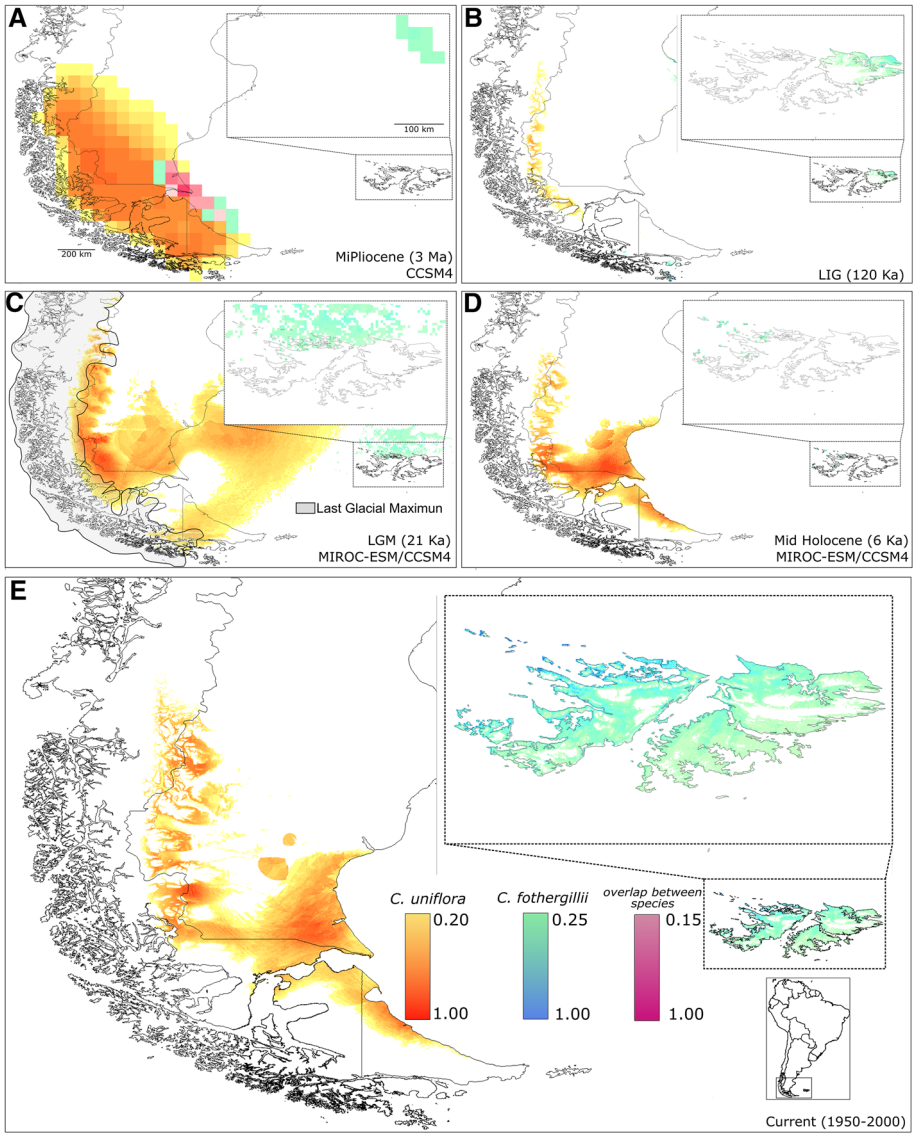


Fig. 6 Spatial projections of *C. uniflora* and *C. fothergillii*'s climatic niche of across several Pliocene and Quaternary climatic scenarios. **a** Mid-Pliocene (3 Mya; CCMS). **b** Last Interglacial maximum (LIG; 120 Mya; CCMS). **c** Last Glacial Maximum (LGM; 21 Kya; average of CCMS and MIROC), dotted lines: ice sheet extent. **d** Mid-Holocene (6 Kya, averages of CCMS and MIROC). **e** Current conditions. Orange hues: suitabilities for *C. uniflora*; blue hues: suitabilities for *C. fothergillii*; pink hues: overlapping high suitabilities

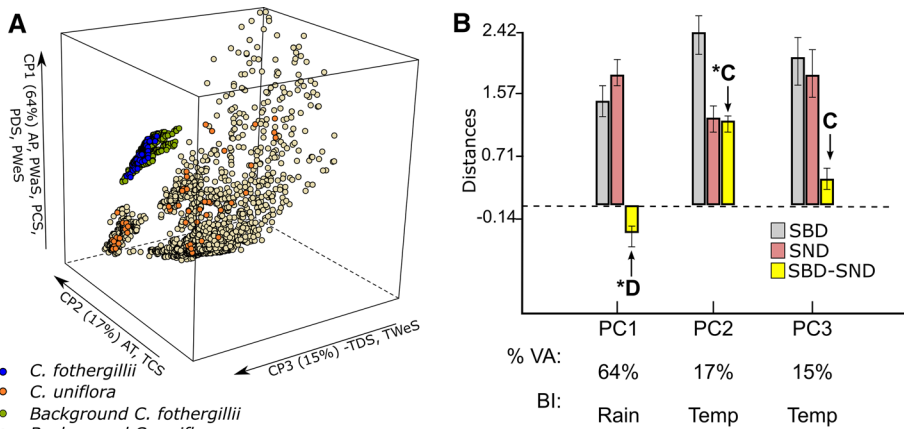


Fig. 7 **a** Comparison of independent niche axes with niche distances of *Calceolaria uniflora* and *C. fothergillii*. Bold letters indicate significant niche divergence (D) or conservatism (C) compared to null distribution based on background divergence between their respective geographic ranges. SBD=species background distance, SND=species niche distance, SBD-SND=difference between species background and niche distances. **b** triplot of the first three climatic principal components showing background and occupancy of the climatic space for the two study species. Variables contributing most to each component are shown on the PC axes

and PC3 showed no significant differences between the observed niches mean distance and the null background distribution (Fig. 7b).

Discussion

Climatic niche divergence and a possible speciation scenario

We integrated phylogeography and niche modelling to provide insights into the geographic context of speciation and the processes driving divergence (Camargo et al. 2010). The paleo-distribution reconstruction based on climatic variables across time clearly showed the sequential spatial differentiation of suitable geographic range from the ancestral lineage to *C. uniflora* and *C. fothergillii* present lineages. According to the paleo-distribution model for mid-Pliocene (~3.3–3.0 Mya), the western and southern areas of continental Patagonia were zones of high climatic suitability for a possible species ancestor. These areas almost reached the Pacific coast and completely covered the island of Tierra del Fuego, which is consistent with the proposed ancestral geographic area being located around latitude 50°–51°S by the Bayesian spatio-temporal diffusion analyses. However, during the mid-Pliocene the species were not yet differentiated; the past projection for this period (according to current niches for both species) appear to overlap only in the mainland, suggesting common climatic requirements at that time, and a continuous divergence since then.

According to the Bayesian spatio-temporal diffusion analyses, divergence between *C. uniflora* and *C. fothergillii* would have occurred around 1.2–1.8 and 0.830–1.25 Ma for the cpDNA and nDNA, respectively. This date is contemporaneous to the GPG, which produced significant environmental changes, increased continentality and affected the distribution of species and taxa composition (Rabassa et al. 2011). Unfortunately, no climatic

layers exist for this glacial period, but as shown by the PDMs for other glacial periods, during the GPG, genetic lineages would have moved eastwards into regions with optimal climatic conditions in the newly exposed areas. During the interglacial period after the GPG, islands and mainland became fully isolated (Ponce et al. 2011; Rabassa et al. 2011), which eliminated gene flow and resulted in species divergence. Because our analysis of climatic niche differentiation suggests that the precipitation regimes, both annual and seasonal, explain the niche differences between species even when considering the background environmental divergence, we suggest evidence exists for incipient climatic niche differentiation, instead of drift-only divergence (McCormack et al. 2009). We also find evidence suggesting that species would have retained similar temperature requirements over time and space. Several studies support the idea that climatic niche conservatism may be important in setting range limits (reviewed in Wiens 2011; Hua and Wiens 2013). Species range limits are set by unsuitable abiotic and/or biotic conditions at their range margins, and the failure of individuals to adapt to those unsuitable conditions (Gaston 2009). Our results suggest that the ancestor of *C. uniflora*–*C. fothergillii* could expand its range across the precipitation axis, adapting to new and diverging conditions, but individuals failed to adapt to unsuitable temperature conditions and thus retained similar temperature requirements. Because range limits create biogeographic patterns, and ecological niches create range limits (reviewed in Wiens 2011), a question for future studies in Patagonian species is if it is possible to identify environmental variables that are conserved across different species, versus those associated with niche divergence and thus suspected to be involved in diversification processes (Espindola et al. 2016).

Intraspecific diversification after speciation

During glacial periods, the distribution ranges of species from lower latitudes in temperate zones contracted, persisting in refugia located at lower elevations or latitudes (Noguerales et al. 2017). Conversely, populations from cold-tolerant species expanded during glacial periods and shrank during interglacials (Stewart et al. 2010; Noguerales et al. 2017). For the Patagonian organisms, there is evidence of periglacial refugia or even more in situ persistence in lands covered by ice, as expected for cold-tolerant species (review Sérsic et al. 2011). However, the question of whether demographic/spatial expansion and contraction have been associated to glacial or interglacial periods is less clear for Patagonian species.

According to our genetic and climatic analysis, the cold-adapted *Calceolaria uniflora* originated, dispersed and diversified in continental Patagonia during the late Quaternary (1 Mya–675 Kya) indicating the profound effect of past climatic oscillations in its abundance, distribution and diversification. The PDMs analyses suggested that during interglacials the range of *C. uniflora* contracted, while during the LGM, this species expanded its range towards central and northern portions of the Patagonian steppe and the merged continental platform that connected mainland to the Malvinas/Falkland Islands. This pattern of spatial expansion during glaciation revealed by the PDMs was also supported by the diffusion analysis, and seems to be accompanied with a demographic expansion occurred at the beginning of the last glacial period OIS6 (ca. 40 Kya; Rabassa 2008).

Interestingly, our analyses revealed two main favourable climatic areas where the species would have persisted across time: an ancient refugial area into the Andean foothills, and a more recent one in a in the Patagonian steppe; the east–west distribution of the main genetic groups coastal refugium retrieved by our cpDNA and nDNA datasets, the secondary contact areas, clearly evidenced by cpDNA and nDNA nucleotide diversity, and the diffusion analyses indicate that successive geographic expansions, isolations and secondary

contacts occurred during glacial/interglacial periods between both areas. Additionally, our genetic results suggest differences in population size, connectivity and reproductive patterns between both refugia. Several lines of evidence (i.e. PDMs, the high genetic diversity, nDNA heterozygosity, and the demographic and diffusion analyses) support the idea that *C. uniflora* persisted since the GPG in the southwestern Andean grassland in a large stable refugium under high gene flow and outcrossing within this area. Conversely, refugia formed since the LGM in the eastern displayed no nDNA genetic diversity probably due to the presence of small populations with high levels of genetic drift and selfing (all sampled individuals were homozygotes). The EBSF suggest that the eastern area was more unstable than the western refugia. Moreover, in the eastern refugia a historical differentiation to the north and south of the Coig river was suggested based on SAMOVA results and haplotype distribution. Interestingly, this genetic break was previously reported in the Patagonian *Anarthrophyllum desideratum* (Cosacov et al. 2013). Thus, the eastern refugia probably consisted of fragmented populations with low connectivity, as revealed by the interpopulation differentiation in chloroplast haplotypes.

In synthesis, we distinguished two main refugial areas located at the east and west of southern geographic distribution range of *C. uniflora*. Both refugial areas are consistent with those previously reported (Cosacov et al. 2010; Sérsic et al. 2011; Nicola et al. 2014; Lopez and Bonasora 2017). From the molecular and climatic evidence, we suggest that both areas would have acted as refugia with different ancientness, geographic extents, population sizes, and reproductive patterns. The contrasting patterns in the distribution of the genetic diversity for both markers could be reflecting different temporal signals (e.g. Mathiasen and Premoli 2010), or could be the result of their different mutation rates, effective population sizes, and/or dispersal mechanisms.

In *C. fothergillii*, each of the markers resulted in different genetic signals. The multilocus species tree retrieved *C. fothergillii* as monophyletic in a moderate-supported clade. Additionally, the paleo-distribution models, and species divergence times, largely support the hypothesis of land bridges between the mainland and the islands during the GPG period. Unlike the cpDNA, the nuclear marker did not differentiate *C. fothergillii* from *C. uniflora*. The lack of genetic differentiation for *C. fothergillii* when using nDNA could be a consequence of several joint processes: (1) colonization of the islands by a small group of continental individuals involved founder effects with limited genetic variation among the founding individuals; (2) by the larger effective population size in nuclear regions, the chance of drift fixing mutations in different populations is lower for nuclear DNA than for chloroplast regions; (3) *C. fothergillii* experienced a bottleneck during milder climatic conditions that reduced genetic diversity in the islands, as predicted by the paleo-distribution models for the interglacial periods; and (4) existence of less outcrossing by pollinators, with no gene flow between continental and insular sites. Regarding this last point, out of the eight pollinating birds observed on *C. uniflora* (Sérsic and Cocucci 1996; Sérsic and Cocucci unpublished data), only the species *Turdus falcklandii* (the Austral Thrush), reaches the Malvinas/Falkland islands. Interestingly, Campagna et al. (2012) have found that *T. falcklandii* would be a resident in the islands since the late Pleistocene, around 44.5 Kya (i.e. before the LGM), and that insular populations not share haplotypes with continental individuals of the species, suggesting no gene flow between the two regions.

Conclusions

The combination of independent data sets (climatic and molecular) points to several factors driving genetic differentiation and speciation in two *Calceolaria* sister species inhabiting continental Patagonia and Malvinas/Falkland islands. Quaternary glacial fluctuations affected the mainland/islands connections favouring speciation. Climatic niche comparisons support both divergence and conservatism of the climatic niche. Future studies including additional molecular markers and other analytical approaches (i.e. the bayesian ABC) in populations of both species, and other species, will help further illuminate the process of lineage differentiation and speciation mechanisms occurring in Patagonia and the Malvinas/Falklands Islands during the Quaternary.

Acknowledgements A. C. and A. N. S. acknowledge the National Research Council of Argentina (CONICET) and the Universidad Nacional de Córdoba (UNC) as researchers, and M. C. B. as postdoctoral fellowship holder. We thank APN Argentina for permits to work within parks and reserves. The authors thank P. R. Riquez for allowing sampling in Ea. Verdadera Argentina, R. Upson, and the Falkland Conservation for providing samples and information on *C. fothergillii*, E. Dominguez for providing georeferences in Chile, A.A. Cocucci, S. Benitez Vieyra D. Carmona for field assistance, and M. C. Acosta for analytical support. Funding: National Research Council of Argentina [PIP 201101-00245, PIP 11220150100690CO] to A.N.S., the National Ministry of Science and Technology [FONCYT-PICT-2011-0837, PICT 2015-3089] to A.N.S., and A.E. was supported by the Swiss National Science Foundation [Grants P300P3 151141 and PBNEP3 140192]

Compliance with ethical standards

Conflict of interest The authors declare no conflicts of interest.

References

- Alsos IG, Engelskjøn T, Gielly L, Taberlet P, Brochmann C (2005) Impact of ice ages on circumpolar molecular diversity: insights from an ecological key species. *Mol Ecol* 14:2739–2753
- Anderson RP, Gonzales I Jr (2011) Species-specific tuning increases robustness to sampling bias in models of species distributions: an implementation with Maxent. *Ecol Model* 222:2796–2811
- Arroyo MTK, Squeo F (1990) Relationship between plant breeding systems and pollination. In: Kawano S (ed) *Biological approaches and evolutionary trends in plants*. Academic Press, London, pp 205–227
- Bandelt HJ, Forster P, Röhl A (1999) Median-joining networks for inferring intraspecific phylogenies. *Mol Biol Evol* 16:37–48
- Baranzelli MC, Cosacov A, Ferreiro G, Johnson L, Sérsic AN (2017) Travelling to the south: Phylogeographic spatial diffusion model in *Monttea aphylla* (Plantaginaceae), an endemic plant of the Monte Desert. *PLoS ONE* 12:0178827
- Barve N (2008) Tool for partial ROC. Biodiversity Institute, Lawrence, KS
- Bielejec F, Rambaut A, Suchard MA, Lemey P (2011) SPREAD: spatial phylogenetic reconstruction of evolutionary dynamics. *Bioinformatics* 27:2910–2912
- Bielejec F, Baele G, Vrancken B et al (2016) Spread3: interactive visualization of spatiotemporal history and trait evolutionary processes. *Mol Biol Evol* 33:2167–2169
- Bouckaert RR (2010) DensiTree: making sense of sets of phylogenetic trees. *Bioinformatics* 15:1372–1373
- Braunisch V, Coppes J, Arlettaz R et al (2013) Selecting from correlated climate variables: a major source of uncertainty for predicting species distributions under climate change. *Ecography* 36:971–983
- Bulgarella M, Kopuchian C, Di Giacom AS et al (2013) Molecular phylogeny of the South American sheld geese with implications for conservation of Falkland islands (Malvinas) and continental populations of the Ruddy-headed Goose *Chloephaga rubidiceps* and Upland Goose *C. picta*. *Bird Conserv Int* 24:59–71
- Camargo A, Sinervo B, Sites JW Jr (2010) Lizards as model organisms for linking phylogeographic and speciation studies. *Mol Ecol* 19:3250–3270

- Camargo A, Werneck F, Morando M, Sites JW Jr, Avila L (2013) Quaternary range and demographic expansion of *Liolaemus darwini* (Squamata: Liolaemidae) in the Monte Desert of Central Argentina using Bayesian phylogeography and ecological niche modelling. *Mol Ecol* 22:4038–4054
- Campagna L, St Clair JH, Loughheed SC et al (2012) Divergence between passerine populations from the Malvinas—Falkland islands and their continental counterparts: a comparative phylogeographical study. *Biol J Linn Soc* 106:865–879
- Comes HP, Kadereit JW (1998) The effect of Quaternary climatic changes on plant distribution and evolution. *Trends Plant Sci* 3:432–438
- Cosacov A, Sérsic AN, Sosa V et al (2009) New insights into the phylogenetic relationships, character evolution, and phytogeographic patterns of *Calceolaria* (Calceolariaceae). *Am J Bot* 96:2240–2255
- Cosacov A, Sérsic AN, Sosa V et al (2010) Multiple periglacial refugia in the Patagonian steppe and post-glacial colonization of the Andes: the phylogeography of *Calceolaria polyrhiza*. *J Biogeogr* 37:1463–1477
- Cosacov A, Johnson L, Paiaro V, Cocucci A, Córdoba FE, Sérsic AN (2013) Precipitation rather than temperature influenced the phylogeography of the endemic shrub *Anarthrophyllum desideratum* in the Patagonian steppe. *J Biogeogr* 40:168–182
- Doyle JJ, Doyle JL (1987) A rapid DNA isolation procedure from small quantities of fresh leaf tissues. *Phytochem Bull* 19:11–15
- Drummond AJ, Suchard MA, Xie D et al (2012) Bayesian phylogenetics with BEAUti and the BEAST 1.7. *Mol Biol Evol* 29:1969–1973
- Dupanloup I, Schneider S, Excoffier L (2002) A simulated annealing approach to define the genetic structure of populations. *Mol Ecol* 11:2571–2581
- Ehrhart C (2000) Die Gattung *Calceolaria* (Scrophulariaceae) in Chile. *Biblioth Bot* 153:1–283
- Excoffier L (2004) Patterns of DNA sequence diversity and genetic structure after a range expansion: lessons from the infinite-island model. *Mol Ecol* 13:853–864
- Excoffier L, Laval G, Schneider S (2005) Arlequin ver. 3.0: an integrated software package for population genetics data analysis. *Evol Bioinform* 1:47–50
- Fernández RJ, Golluscio RA, Bisigato AJ et al (2002) Gap colonization in the Patagonian semidesert: seed bank and diaspore morphology. *Ecography* 25:336–344
- Fu YX (1997) Statistical tests of neutrality of mutations against population growth, hitchhiking and background selection. *Genetics* 147:915–925
- Gaston KJ (2009) Geographic range limits: achieving synthesis. *Proc R Soc B* 276:1395–1406
- Hall TA (1999) BioEdit: a user-friendly biological sequence alignment editor and analysis program for Windows 95/98/NT. *Nucleic Acids Symp Ser* 41:95–98
- Hamilton MB (1999) Four primer pairs for the amplification of chloroplast intergenic regions with intraspecific variation. *Mol Ecol* 8:521–523
- Heled J, Drummond AJ (2008) Bayesian inference of population size history from multiple loci. *BMC Evol Biol* 8:289
- Heled J, Drummond AJ (2010) Bayesian inference of species trees from multilocus data. *Mol Biol Evol* 27:570–580
- Hewitt GM (2004) Genetic consequences of climatic oscillations in the quaternary. *Philos Trans Ser B* 359:183–195
- Hijmans RJ, Cameron SE, Parra JL et al (2005) Very high resolution interpolated climate surfaces for global land areas. *Int J Climatol* 25:1965–1978
- Hua X, Wiens JJ (2013) How does climate influence speciation? *Am Nat* 182:1–12
- Karl SA, Avise JC (1993) PCR-based assays of Mendelian polymorphisms from anonymous single-copy nuclear DNA: techniques and applications for population genetics. *Mol Biol Evol* 10:342–361
- Kébé K, Alvarez N, Tuda M et al (2017) Global phylogeography of the insect pest *Callosobruchus maculatus* (Coleoptera: Bruchinae) relates to the history of its main host, *Vigna unguiculata*. *J Biogeogr* 44:2515–2526
- Lemey P, Rambaut A, Welch JJ et al (2010) Phylogeography takes a relaxed random walk in continuous space and time. *Mol Biol Evol* 27:1877–1885
- Lessa EP, D'Elía G, Pardiñas UFJ (2010) Genetic footprints of late quaternary climate change in the diversity of Patagonian-Fueguian rodents. *Mol Ecol* 19:3031–3037
- Librado P, Rozas J (2009) DnaSP v5: a software for comprehensive analysis of DNA polymorphism data. *Bioinformatics* 25:1451–1452
- Lima-Ribeiro MS, Varela S, González-Hernández J et al (2015) Ecoclimate: a database of climate data from multiple models for past, present, and future for macroecologists and biogeographers. *Biodivers Inform* 10:1–21
- Lopez A, Bonasora MG (2017) Phylogeography, genetic diversity and population structure in a Patagonian endemic plant. *Ann Botany* 9:plx017

- Losos JB, Ricklefs RE (2009) Adaptation and diversification on islands. *Nature* 457:830–836
- Mascó M, Noy-Meir I, Sérsic AN (2004) Geographic variation in flower color patterns within *Calceolaria uniflora* Lam. in Southern Patagonia. *Plant Syst Evol* 244:77–91
- McCormack JE, Zellmer AJ, Knowles LL (2009) Does niche divergence accompany allopatric divergence in *Aphelocoma* jays as predicted under ecological speciation?: insights from tests with niche models. *Evolution* 64:1231–1244
- McDowall RM (2005) Falkland Islands biogeography: converging trajectories in the South Atlantic Ocean. *J Biogeogr* 32:49–62
- Molau U (1988) Scrophulariaceae—Part I. Calceolariaceae. *Flora Neotropica* 47:1–326
- Morrone JJ, Posada P (2005) Falklands: facts and fiction. *J Biogeogr* 32:2183–2187
- Nascimento FF, Lazar A, Menezes AN et al (2013) The role of historical barriers in the diversification processes in open vegetation formations during the Miocene/Pliocene using an ancient rodent lineage as a model. *PLoS ONE* 8:e61924
- Nei M (1987) *Molecular evolutionary genetics*. Columbia Univ. Press, New York
- Nicola MV, Sede SM, Pozner R et al (2014) Phylogeography and palaeodistribution modelling of *Nassauvia* subgenus *Strongyloma* (Asteraceae): exploring phylogeographical scenarios in the Patagonian steppe. *Ecol Evol* 4:4270–4286
- Noguerales V, Cordero PJ, Ortego J (2017) Testing the role of ancient and contemporary landscapes on structuring genetic variation in a specialist grasshopper. *Ecol Evol* 7:3110–3122
- Nylinder S, Swanson U, Persson C et al (2012) A dated species-tree approach to the trans-Pacific disjunction of the genus *Jovellana* (Calceolariaceae, Lamiales). *Taxon* 61:381–391
- Otto-Bliesner BL, Marshall SJ, Overpeck JT et al (2006) Simulating arctic climate warmth and icefield retreat in the last interglaciation. *Science* 311:1751–1753
- Papadopoulou A, Jones AG, Hammond PM et al (2009) DNA taxonomy and phylogeography of beetles of the Falkland Islands (Islas Malvinas). *Mol Phylogenet Evol* 53:935–947
- Peterson AT, Papes M, Soberón J (2008) Rethinking receiver operating characteristic analysis applications in ecological niche modeling. *Ecol Model* 213:63–72
- Pfanzelt S, Albach DC, von Hagen KB (2017) *Tabula rasa* in the patagonian channels? The phylogeography of *Oreobolus obtusangulus* (Cyperaceae). *Mol Ecol* 26:4027–4044
- Phillips SJ, Anderson RP, Schapire RE (2006) Maximum entropy modeling of species geographic distributions. *Ecol Model* 190:231–259
- Ponce JF, Rabassa J, Coronato A, Borromei AM (2011) Palaeogeographical evolution of the atlantic coast of pampa and patagonia from the last glacial maximum to the Middle Holocene. *Biol J Linn Soc* 103:363–379
- QGIS Development Team (2016) QGIS geographic information system. Open source geospatial foundation project. Available from <http://www.qgis.org/>. Accessed Dec 2016
- Rabassa J (2008) Late Cenozoic glaciations in Patagonia and Tierra del Fuego. In: Rabassa J (ed) *The late Cenozoic of Patagonia and Tierra del Fuego*. Elsevier, Oxford, pp 151–204
- Rabassa J, Coronato A, Martínez O (2011) Late Cenozoic glaciations in Patagonia and Tierra del Fuego: an updated review. *Biol J Linn Soc* 103:316–335
- Rambaut A, Drummond AJ (2008) FigTree: tree figure drawing tool, v1.2.2. Institute of Evolutionary Biology, University of Edinburgh. <http://tree.bio.ed.ac.uk/software/figtree>
- Rambaut A, Drummond AJ (2009) Tracer, v1.5.0. MCMC trace analysis tool. <http://beast.bio.ed.ac.uk/Tracer>. Accessed Dec 2016
- Ramos VA, Ghiglione J (2008) Tectonic evolution of the Patagonian Andes. In: Rabassa J (ed) *The late Cenozoic of Patagonia and Tierra del Fuego*. Elsevier, Oxford, pp 57–71
- Rull V (2006) Quaternary speciation in the neotropics. *Mol Ecol* 15:4257–4259
- Ruzzante DE, Walde SJ, Gosse JC et al (2008) Climate control on ancestral population dynamics: insight from patagonian fish phylogeography. *Mol Ecol* 17:2234–2244
- Sérsic AN (2004) Pollination biology in the genus *Calceolaria* L. (Calceolariaceae). *Stapfia* 82:1–125
- Sérsic AN, Cocucci AA (1996) A remarkable case of ornithophily in *Calceolaria*: food bodies as rewards for a non-nectarivorous bird. *Bot Acta* 109:172–176
- Sérsic AN, Cosacov A, Cocucci AA et al (2011) Emerging phylogeographical patterns of plants and terrestrial vertebrates from Patagonia. *Biol J Linn Soc* 103:475–494
- Shaw J, Lickey EB, Beck JT et al (2005) The tortoise and the hare II: relative utility of 21 noncoding chloroplast DNA sequences for phylogenetic analysis. *Am J Bot* 92:142–166
- Simmons MP, Ochoterena H (2000) Gaps as characters in sequence-based phylogenetic analyses. *Syst Biol* 49:369–381
- Singer B, Ackert R, Guillou H (2004) 40Ar/39Ar and K-Ar chronology of pleistocene glaciations in Patagonia. *GSA Bull* 116:434–450

- Stephens M, Smith NJ, Donnelly P (2001) A new statistical method for haplotype reconstruction from population data. *Am J Hum Genet* 68:978–989
- Stewart JR, Lister AM, Barnes I (2010) Refugia revisited: individualistic responses of species in space and time. *Proc R Soc Lond B* 277:661–671
- Tajima F (1983) Evolutionary relationship of DNA sequences in finite populations. *Genetics* 105:437–460
- Tajima F (1989) The effect of change in population size on DNA polymorphism. *Genetics* 123:598–601
- Thompson JD, Gibson TJ, Plewniak F et al (1997) The ClustalX windows interface: flexible strategies for multiple sequence alignment aided by quality analysis tools. *Nucleic Acids Res* 24:4876–4882
- Upton R, McAdam JH, Broughton DA et al (2012) *Calceolaria fothergillii*. The IUCN Red List of Threatened Species 2012: e.T15245657A15245660
- Vuilleumier F (1991) A quantitative survey of speciation phenomena in Patagonian birds. *Ornitol Neotr* 2:5–28
- Watson DF (1992) *Contouring: a guide to the analysis and display of spatial data*. Pergamon Press, New York
- Werneck FP, Leite RN, Geurgas SR (2015) Biogeographic history and cryptic diversity of saxicolous Tropiduridae lizards endemic to the semiarid Caatinga. *BMC Evolution Biol* 15:94
- Wiens JJ (2011) The niche, biogeography and species interactions. *Philos Trans R Soc London B* 366:2336–2350